Elsevier Editorial System(tm) for Industrial Crops and Products

Manuscript Draft

Manuscript Number: INDCRO-D-20-00846R3

Title: Enhancement of the nanofibrillation of birch cellulose pretreated with natural deep eutectic solvent

Article Type: Research Paper

Section/Category: Fibres, proteins and carbohydrates

Keywords: deep eutectic solvent; birch cellulose; sustainable; cellulose nanofiber

Corresponding Author: Dr. Hailan Lian, Ph.D.

Corresponding Author's Institution: Nanjing Forestry University

First Author: Shu Hong

Order of Authors: Shu Hong; Yang Yuan; Panpan Li; Kaitao Zhang; Hailan Lian, Ph.D.; Henrikki Liimatainen, Ph.D

Abstract: In this study, we demonstrate a new bio-derived and non-toxic deep eutectic solvent composed of betaine hydrochloride (Bh) and glycerol (Gl) as a pretreatment medium for birch cellulose (Betula pendula) to prepare cellulose nanofibers (CNFs) using microfluidization. The co-solvent could readily penetrate into cellulose to swell the fibrillar structure and weaken the interaction within the hydrogen bond network. Moreover, the cationization of glycerol and cellulose by betaine hydrochloride further enhances the swelling process. All of these effects promote the nanofibrillation of cellulose and reduce the energy demand in CNF production. A high CNF mass yield of up to 72.5% was obtained through co-solvent pretreatment using a Bh-to-Gl mole ratio of 1:2 at 150°C for 1 h. The mole amount of betaine hydrochloride was noted to affect the nanofibrillation process and stability of the CNF suspension. The obtained CNFs possessed a cationic charge of 0.05-0.06 mmol/g, a diameter of 17-20 nm, and a degree of crystallinity of 67.7-74.4%. The CNFs displayed good thermal stability comparable to that of the pristine cellulose. Thus, this study provides a green and efficient swelling strategy for producing CNFs with a low cationic charge density.

Dear Editor in chief,

Thank you for your letter and for the reviewers' comments concerning our manuscript entitled "Enhancement of the nanofibrillation of birch cellulose pretreated with natural deep eutectic solvent" (INDCRO-D-20-00846R2). All the comments were addressed. And responses to reviewers' comments were listed point-by-point and any changes made in the revised manuscript was informed accordingly. Please see it in our revised manuscript highlighted with red.

We tried our best to improve the manuscript and made some changes in the manuscript. We appreciate for Editors/Reviewers' warm work earnestly and hope that our responses are adequate enough. Thank you for your constructive feedback and comments.

Since this manuscript is important for us, I would be greatly appreciated if I could hear from you soon.

Thank you very much for your consideration.

Yours sincerely,

Hailan Lian

lianhailan@njfu.edu.cn

Paper Title: Enhancement of the nanofibrillation of birch cellulose pretreated with natural deep eutectic solvent

Ms. No.: INDCRO-D-20-00846R2

Dear Editor-in-Chief,

We appreciate the detailed and helpful comments for improving the quality of our manuscript. We have done our best to make the required corrections and truly hope our responses are adequate enough.

The number of pages and lines concerned with the modifications added to the manuscript was informed in the responses to reviewers' comments. And changes were made accordingly.

Responses to editor´s and reviewers' comments are listed point-by-point as below and are shown in **blue**.

We look forward to hearing from you soon.

Comments:

Editor:

-PLEASE USE A FONT OTHER THAN BLACK TO INDICATE THE REVISED PARTS OF YOUR MANUSCRIPT.

Response: We used **red font** to indicate the revised parts in the manuscript.

-Please check if all responses to reviewers, in the first version revised, have been addressed in the revised manuscript, and add those that have not been addressed. Please note that future readers could have the same questions as reviewers.

Response: Checked.

-Please inform the number of pages and lines concerned with the modifications added to the manuscript.

Response: The pages and lines are informed in response to reviewers' comments, where changes were made.

-Please make sure that in addition to having responded to the questions and comments, you have also made all the changes in the manuscript accordingly.

Response: Checked.

-Please note that your resubmission will be subject to re-review before a decision is rendered.

Reviewer #1: It is important that the detailed explanation about experiments to be added to the manuscript.

Response: We have added more detailed explanation about experiments in the revised manuscript. Page 6, line 103-104; Page 7, line 136, line 139, line 140, line 144-145; Page 9, line 183.

Reviewer #3:

Authors have addressed my comments.

However, I asked the authors to incorporate images of the different suspensions to corroborate how homogeneity was assessed.

This image has been provided in the response to reviewers document, but not in the manuscript.

I consider that this needs to be incorporated into the manuscript.

Response: Now, we put it in the revised supporting information. As we informed in page 10, line 213. In supporting information Figure S1 was inserted accordingly, Page 2, line 11-14.

Reviewer #4: I appreciate authors' effort to revise the manuscript and answer to reviewers' comments.

-In abstract (line #11) : It is recommended to change "a new cost-effective and safe deep eutectic solvent" to "a new bio-derived and non-toxic deep eutectic solvent".

Response: Thank you for your suggestion, we have revised this accordingly. Please see it in Page 2, line 10.

- This manuscript shows the possibility of Bh-Gl DES to use as pretreatment for the production of cellulose nanofibrils, but it is thought that their effect is not much greater compared to other DES. Therefore, it is recommended to remove the expression "notable" (line 430). It is better to remove this sentence (line 429-431, "Compared with the common methods used for…advantages".)

Response: We deleted this sentence and revised the statement. Page 19, line 436-437.

- Authors evaluated crystallinity by XRD, and analyzed the structure with NMR analysis. Using NMR results, the crystallinity can be evaluated. Could you compare the crystallinity degree results depending on the measurement method (XRD and NMR)?

Please check the crystallinity if they show similar tendency.

Response: We conducted the NMR analysis for birch cellulose before and after the DES treatment, and the results were used for illustrating the structure changes as shown in Figure 2b. According to the method of solid-state NMR study on cellulose crystallinity (Newman RH, 2004, Holzforschung), the CrI of cellulose was calculated based on sub-spectrum showing peaks assigned to the C4 in cellulose. The CrI is calculated by $CrI=I_{C4,\ cry}/(\ I_{C4,\ cry}+\ I_{C4,\ am})$. The CrIs of birch cellulose and Bh_2Gl_3 were 55% and 50%, respectively. This result also indicated the pretreated birch cellulose showed a lower crystallinity than pristine one. This showed a similar tendency with the result of XRD analysis. The decrease of CrI value of treated birch cellulose was due to the swelling effect of DES on cellulose, which was found similar as in a recent study using choline chloride and imidazole DES as swelling medium for cellulose to make cellulose nanofibers (Sirviö et al, 2020, Green Chemistry). And the introduce esters groups may also have effect on the decrease on CrI value, which is similar as previous study by introducing acetyl groups on chitin (Hong et al, 2019, Carbohydrate Polymers). This part discussion was added in Page 16, line 356-367. In supporting information, Figure S4 was inserted in Page 5, line 21-22.

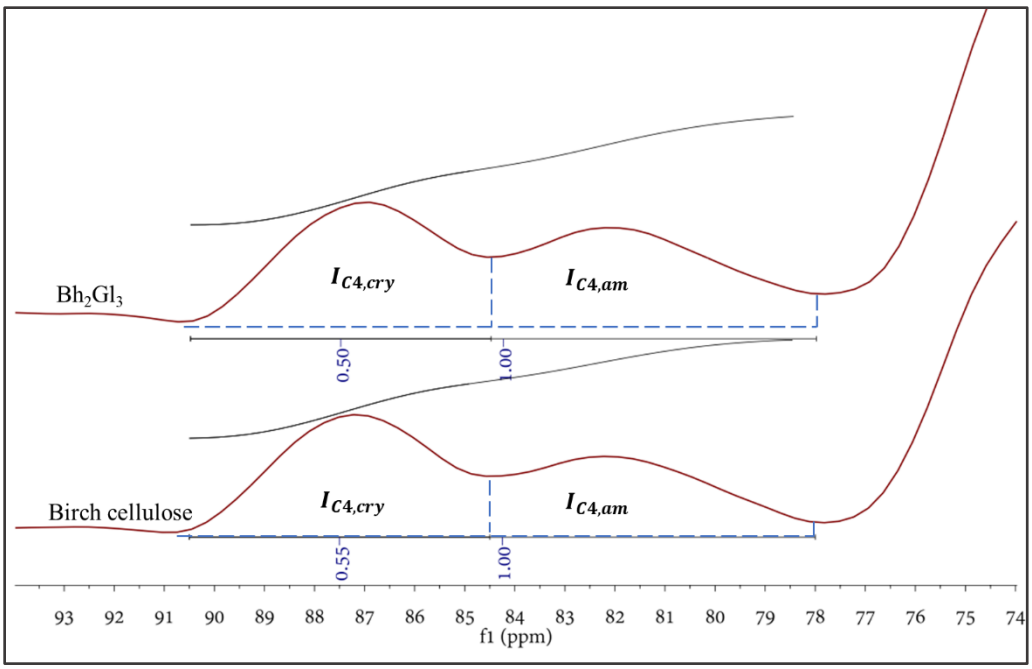

Figure S4. CrI calculation of C4 region in NMR for birch cellulose and Bh_2Gl_3.

Newman RH: Homogeneity in cellulose crystallinity between samples of Pinus radiata wood. Holzforschung 2004, 58:91-96.

Sirviö J A, Hyypio K, Asaadi S, et al. High-strength cellulose nanofibers produced via swelling pretreatment based on a choline chloride–imidazole deep eutectic solvent[J]. Green Chemistry, 2020, 22(5): 1763-1775.

Hong S, Yuan Y, Yang Q, et al. Choline chloride-zinc chloride deep eutectic solvent mediated preparation of partial O-acetylation of chitin nanocrystal in one step reaction[J]. Carbohydrate Polymers, 2019: 211-218.

Graphical Abstract

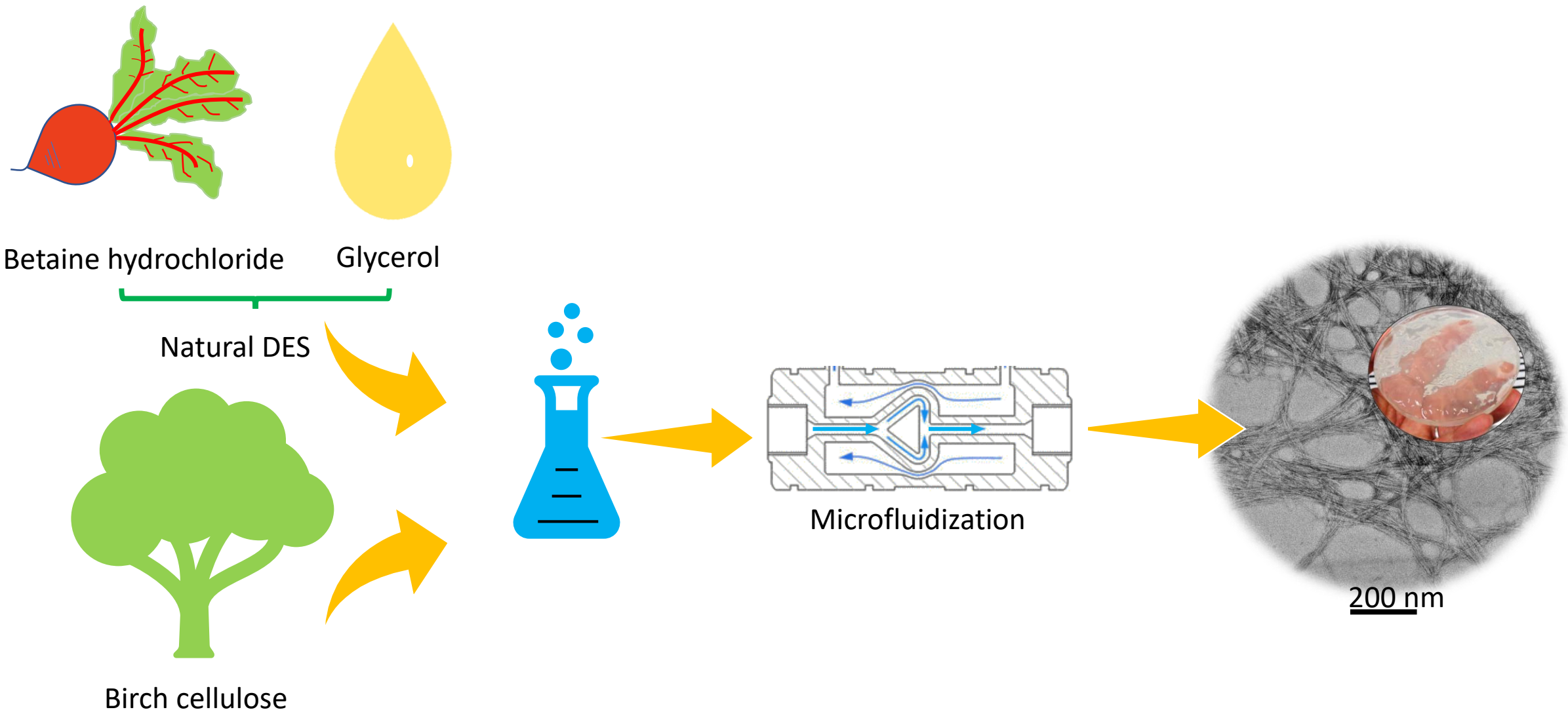

***Highlights (for review)**

- Betaine hydrochloride/ glycerol DES was used for pretreatment of birch cellulose
- The pre-treated cellulose was successfully liberated to CNF with microfluidization
- The surface of obtained CNF was mildly cationized
- The main chemicals used here are all natural products

Enhancement of the nanofibrillation of birch cellulose pretreated with natural deep eutectic solvent

Shu Hong,[a, b] *Yang Yuan,*[a] *Panpan Li,*[b] *Kaitao Zhang,*[b] *Hailan Lian,*[*, a] *Henrikki Liimatainen* [*, b]

[a] College of Materials Science and Engineering, Nanjing Forestry University, Nanjing, 210037, China

[b] Fibre and Particle Engineering Research Unit, University of Oulu, P.O. Box 4300, 90014 Oulu, Finland

* Corresponding authors

Hailan Lian, E-mail: lianhailan@njfu.edu.cn and Henrikki Liimatainen, E-mail: Henrikki.Liimatainen@oulu.fi

Abstract: In this study, we demonstrate a new bio-derived and non-toxic deep eutectic solvent composed of betaine hydrochloride (Bh) and glycerol (Gl) as a pretreatment medium for birch cellulose (*Betula pendula*) to prepare cellulose nanofibers (CNFs) using microfluidization. The co-solvent could readily penetrate into cellulose to swell the fibrillar structure and weaken the interaction within the hydrogen bond network. Moreover, the cationization of glycerol and cellulose by betaine hydrochloride further enhances the swelling process. All of these effects promote the nanofibrillation of cellulose and reduce the energy demand in CNF production. A high CNF mass yield of up to 72.5% was obtained through co-solvent pretreatment using a Bh-to-Gl mole ratio of 1:2 at 150°C for 1 h. The mole amount of betaine hydrochloride was noted to affect the nanofibrillation process and stability of the CNF suspension. The obtained CNFs possessed a cationic charge of 0.05–0.06 mmol/g, a diameter of 17–20 nm, and a degree of crystallinity of 67.7–74.4%. The CNFs displayed good thermal stability comparable to that of the pristine cellulose. Thus, this study provides a green and efficient swelling strategy for producing CNFs with a low cationic charge density.

Keywords: deep eutectic solvent, birch cellulose, sustainable, cellulose nanofiber

1. Introduction

Over the last few decades, the harnessing of cellulose as a green source for designing various every-day commodities and novel advanced applications has gained much attention. The sources of cellulose are widely distributed in nature from plant cells to bacterial. Nanoscale cellulose materials have been considered as inexhaustible and especially promising high-performing future materials (Habibi et al., 2010). As a natural green renewable material, nanocellulose can be structured as an end product that has high transparency, is lightweight, and has very good mechanical properties with the desired chemical functionality (Siró and Plackett, 2010). So far, cellulose nanomaterials have been demonstrated as, for example, reinforcements in a polymer matrix (Chen et al., 2017, 2018a), tissue scaffolds (Lin and Dufresne, 2014), conductive or energy storage materials (Li et al., 2015; Chen et al., 2018b), Pickering emulsions (Ojala et al., 2016; Laitinen et al., 2017), and barrier materials (Siró and Plackett, 2010; Wu et al., 2012).

Production of nanocellulose (excluding bacterial nanocellulose) is based on top-down techniques in which raw cellulose material is disintegrated down to its nanoscale constituents. In particular, the liberation of elongated cellulose nanofibers (CNFs) requires intensive mechanical treatments (Siró and Plackett, 2010; Carvalho et al., 2019). To decrease the energy consumption, various pre-treatments (e.g., alkaline swelling (Bhatnagar and Sain, 2005), enzymatic hydrolysis (Pääkkö et al., 2007), and chemical derivatization (Saito et al., 2006)) that are applied to enhance the nanofibrillation process. The internal structure of cellulose fibers was compacted through hydrogen bond and it is hard to react with chemicals. However, there is still large amount of more reactive hydroxyl groups on the surface of cellulose. The hydroxyl groups of cellulose can, for instance, be esterified (Braun and Dorgan, 2009) or oxidized to carboxyl (Saito et al., 2006) or aldehyde groups (Liimatainen et al., 2012, 2013; Sirviö et al., 2014), which

allows weakening the recalcitrant interfibrillar hydrogen bond network of cellulose and to facilitate the nanofibrillation process.

Deep eutectic solvents (DESs) are self-associated liquid mixtures that typically consist of a hydrogen bond donor (HBD) and hydrogen bond acceptor (HBA) pair and can be tailored by adjusting the properties of the HBD and HBA. Typically, the freezing point of DESs is below 100 °C (Smith et al., 2014), and lower than their individual constituents. They are often considered to be ionic liquid (IL) analogues, which exhibit both low vapor pressure and a good solvent capability for chemical synthesis (Mota-Morales et al., 2018; Hong et al., 2020b). Compared to ILs, DESs are commonly less costly, more commercially available, and easier to prepare (Abbott et al., 2004; Hong et al., 2019b). Since the DESs can interact with hydrogen bond systems, they have widely been viewed as low-toxic and biodegradable green solvents in biomass and polysaccharide processing (Vigier et al., 2015; Zdanowicz et al., 2018; Hong et al., 2018). DESs have also been applied in the fabrication of functionalized cellulose nanomaterials. For example, urea-based DESs have been used as a pretreatment in the production of CNFs through mechanical disintegration (Sirviö et al., 2015; Li et al., 2017). However, urea has been found to react with cellulose to form carbamates at high temperatures in acidic conditions (Willberg-Keyriläinen et al., 2018). Acidic DESs, in turn, have been used as a hydrolytic medium for the production of cellulose nanocrystals (CNCs) (Sirviö et al., 2016). More recently, acidic and alkaline DESs were used to the systematic fraction of biomass, and the obtained cellulose rich part was further coupled with mechanical treatment for production of lignin containing nanocellulose (Suopajärvi et al., 2020; Hong et al., 2020a). DESs show great potential in pretreatment of (ligno)cellulose for fabrication of nanocellulose or lignin containing nanocellulose.

Glycerol is a simple natural polyol that is inexpensive and biodegradable. It is nontoxic and widely used in the food industry. Glycerol is generally obtained from plant and animal sources, where it occurs in triglycerides, which are esters of glycerol with long-chain carboxylic acids. The hydrolysis, saponification, or transesterification of these triglycerides produces glycerol as well as the fatty acid derivatives. Therefore, glycerol can be considered as a green and sustainable solvent (Hong et al., 2019a). Previously, glycerol has been directly used as a wetting agent or a hydrolytic pretreatment medium in the presence of sulfuric acid for the preparation of CNFs and CNCs (Lu et al., 2019; Ramakrishnan et al., 2019). However, relatively harsh reaction conditions, with a treatment temperature and time of 120–200 °C and 3–4 h, respectively, were applied.

In this study, a DES based on betaine hydrochloride (Bh) and glycerol (Gl) was used as the pretreatment medium for enhancing the nanofibrillation of birch cellulose to product CNF. Betaine hydrochloride was selected due to its natural availability and its ability to release hydrochloric acid at a high temperature. The released acid can facilitate the depolymerization of cellulose in the presence of glycerol. Compared with mineral acids, betaine hydrochloride is more sustainable, more biodegradable, and easier to handle, and it could enable simultaneous cationization of cellulose. Different pretreatment conditions were explored, including temperature, the mole ratio of the DES constituents, and time. The physicochemical characteristics of DES-treated cellulose and CNF were further analyzed by diffuse reflectance infrared Fourier transform spectroscopy (DRIFTS), thermogravimetric analysis (TGA), X-ray diffraction (XRD), and scanning electron microscopy (SEM) to determine their chemical structure, thermal stability, crystallinity, and surface morphology, respectively. The mechanical properties of CNF were determined by tensile strength measurements from nanocellulose films.

2. Materials and methods

2.1. Materials

The dry sheet of bleached birch pulp (*Betula pendula*) was firstly dispersed in water and washed with deionized (DI) water. After drying at 60 °C for 24 h, it was collected and used as cellulose raw material. The purpose of DI water was used for swelling the cellulose first, which is beneficial for infiltrating and swelling cellulose of DES. The chemical composition (cellulose, xylan, glucomannan, lignin and extractive contents were 74.8%, 23.6%, 1.1%, 0.4% and 0.08%) of pulp and other properties have been presented in our previous study (Liimatainen et al., 2011). Glycerol (97%) was purchased from VWR (France) and betaine hydrochloride from TCI (Germany). All chemicals were used as received, and DI water was used throughout the experiments.

2.2 Preparation of DESs and pretreatment of cellulose in DESs

DESs were prepared with various molar ratios, 1:6, 1:3, 1:2, and 2:3 (HBA to HBD, betaine hydrochloride to glycerol), by mixing the constituent at 100 °C in a beaker. Cellulose was added to the DESs (mass ratio of 1:25) at a given temperature (130, 140, or 150 °C) for a desired time (0.5 or 1 h) under continuous stirring in a beaker. After the treatment, the mixture was cooled at room temperature for 10 min. The pretreated cellulose was then separated by adding water and filtering through 5–13 µm filter paper (VWR, France) and was washed until the filtrate became neutral. The solid residue was collected and diluted to 0.5 wt-% for further mechanical disintegration with a microfluidizer.

2.3 Disintegration of cellulose with microfluidizer

The DES-treated cellulose was disintegrated into nanocellulose with a microfluidizer (Microfluidics M-110EH-30, Westwood, MA, USA) equipped with a double-chamber system (400 and 200 µm), through which the cellulose was cycled in sequence. First, the suspension passed for three cycles at 1000 bar. Half of the suspension was collected and

named CNF I. Then, the remaining volume was passed through the microfluidizer again for three cycles at 1000 bar and named CNF II.

2.4 Characterization of cellulose fibers and CNFs

The degree of polymerization (DP) of the cellulose fibers was calculated based on the limiting viscosity values of the freeze-dried samples. The samples were dissolved into a cupriethylenediamine solution (CED) according to the ISO 5351 standard. The DP was calculated from the limiting viscosity according to Eq. 1(Li et al., 2017):

$$\mathrm{DP} = \left(\frac{1.65[\eta]-116H}{C}\right)^{1.111}, \quad (1)$$

where [η] = the limiting viscosity ($dm^3\ kg^{-1}$), C = the mass fraction of cellulose, and H = the mass fraction of hemicellulose.

SEM (Zeiss Zigma HD VP, Germany) was used to observe the morphology of the cellulose before and after DES treatment with EHT of 5 kV. For nanocellulose, a droplet of 0.01 wt-% CNF suspension was dosed on monocrystalline silicon and dried in an ambient environment for 24 h. Before examination, all samples were deposited with a thin Pt layer under vacuum using a sputter coater for 30 s.

The dimensions of the wet cellulose fibers before and after co-solvent treatment were analyzed using a Valmet fiber image analyzer (Valmet FS5, Valmet, Finland). Approximately 1 g of suspension was added to the plastic beaker, which was diluted by Valmet FS5 automatically to adjust the consistency of the cellulose. Over 100,000 fibers of each samples were captured and analyzed for their width and length. This method can notice typically 0.1 µm differences in fiber dimension.

For the TEM imaging, a droplet of nanocellulose suspension (0.01 wt-%) was directly deposited onto a carbon-coated copper grid and was dried under the ambient conditions for 2 h. After that, excess liquid was removed by blotting with filter paper. Then, samples were stained with a droplet of uranyl acetate (2% w/v) on top of each

specimen for 30 min. The excess solvent was removed with filter paper. The grid was then allowed to fully dry in air for at least 12 h prior to imaging with a Tecnai G2 Spirit transmission electron microscope (TEM, FEI Europe, Eindhoven, Netherlands) at 100 kV accelerating voltage.

Diffuse reflectance infrared Fourier transform spectroscopy (DRIFTS) was used to analyze the chemical structure of the cellulose. The spectra were collected from freeze-dried samples in ambient conditions (Bruker VERTEX 80V spectrometer, USA) using 40 scans at a 2 cm^{-1} resolution in the 600–4000 cm^{-1} range.

Solid-state ^{13}C cross-polarization/magic angle spinning (^{13}C CP/MAS) nuclear magnetic resonance (NMR) spectroscopy was used to obtain detailed information about the chemical structure of the celluloses. The spectra were acquired with a Bruker AVANCE 400WB (Bruker, Germany) spectrometer operating at 100.7 MHz for ^{13}C.

The cationic charge density of the CNFs was determined using the polyelectrolyte titration method with a particle charge detector (BTG Mütek PCD-03, Germany). First, the CNF suspension was diluted with DI water to 0.1 wt-% and was stirred for 0.5 h. Then, 1 ml of the suspension and 9 ml of DI water were added to a polytetrafluoroethylene container and titrated with sodium polyethylene sulfonate (PES-Na, 0.001 N) polyelectrolyte. The charge density was calculated based on the consumption of the polyelectrolytes. Each sample was tested three times.

The crystalline structure of the cellulose was determined by powder XRD using a Bruker D8 ADVANC (Bruker, Germany) with Cu Kα radiation at an operating voltage of 40 kV and a filament current of 30 mA. The data were collected at a scan speed of 5° 2θ/min from 5° to 55°. The crystalline index (CrI; %) was calculated according to Eq. (2) (Segal et al., 1959):

$$\mathrm{CrI} = \left[\frac{I_{200} - I_{am}}{I_{200}}\right] \times 100\,, \qquad (2)$$

where I_{200} is the peak intensity of the main crystalline plane diffraction located at $2\theta \cong 22.7°$ and I_{am} is the intensity of the amorphous diffraction at $2\theta \cong 18°$.

TGA was performed using a Mettler Toledo TGA 2 SF/1100 apparatus (Mettler Toledo, NY, USA). Approximately 3 mg samples were loaded in alumina crucibles. The measurement was carried out in a nitrogen atmosphere with flow rates of 30 mL/min in a temperature range of 30–600 °C at 10 °C/min.

2.5 Preparation and characterization of nanocellulose films

Self-standing films (grammage of ~80 g/m^2) were prepared through vacuum filtration from diluted CNF suspension (0.2 wt-%) with a sand core funnel on a polyvinylidene fluoride (PVDF) membrane (pore size 0.65 μm). The wet sheets were covered by another PVDF film, and the sandwich structure was transferred to a Rapid-Köthen sheet dryer (Karl Schröder KG, Germany) and compressed between two paper sheets at 93 °C under a vacuum at about 800 mbar of pressure for 10 min.

The films were conditioned in the measurement environment (with a relative humidity of 50% at 23 °C) for at least 24 h. Then, they were cut into strips with a dimension of 5 mm in width and 50 mm in length. The thickness of each strip was measured using a precision thickness gauge (Hanatek FT3, UK). At least three points in each sample were measured, and the thickness was averaged. The tensile strength of the nanocellulose films was determined by measuring the tensile stress and strain at breaking with a universal testing machine (Zwick D0724587, Switzerland) equipped with a 100 N load cell (Sirviö, 2019).

3. Results and discussion

3.1 The influence of conditions of co-solvent pretreatment on cellulose characteristics

Previously, betaine hydrochloride has been used as a Bronsted acid catalyst in the production of 5-hydroxymethyfurfural (HMF) in a DES medium (Vigier et al., 2012).

Betaine hydrochloride has also been exploited in the production of ionic building blocks based on glycerol esterification (Journoux-Lapp et al., 2017). Cellulose also is made up of multiple reactive hydroxyl groups. Therefore, it is a highly appealing bio-based chemical for tailoring characteristics of cellulose. However, betaine hydrochloride is a solid and cannot be directly used as a solvent. Glycerol is, in turn, a good solvent for betaine hydrochloride, and it can simultaneously work as a swelling agent for cellulose. In the present work, a co-solvent consisting of betaine hydrochloride and glycerol with different mole ratios (1:6 to 2:3) was used for cellulose pretreatment in different conditions (**Table 1**) to facilitate fabrication of CNFs. Of the screened conditions, only Bh:Gl mole ratios of 1:2 and 2:3 resulted in homogeneous mixtures that promoted cellulose disintegration into stable CNF suspensions. And the other examined reaction conditions resulting in inhomogeneous cellulose suspensions, which showed big fiber particles or flocculation and readily form sediments (The typical images were **Figure S1**). Earlier, pure glycerol was also able to convert cellulose into nanocellulose, but a high temperature of 180–200 °C was required (Ramakrishnan et al., 2019). Thus, betaine hydrochloride played a vital and synergic role here and enabled efficient production of CNF in milder conditions.

To optimize the pretreatment conditions, lower temperature and reaction time were also investigated (see entries 5–7 in Table 1). However, these milder conditions did not lead to stable and well-dispersed nanocellulose suspensions and demonstrated that both reaction temperature and time had a significant effect on the formation of cellulose nanoparticles after mechanical treatment. Moreover, it was noted that CNF samples obtained using mole ratios of 1:2 and 2:3 (entries 3 and 4 in Table 1) were more slurry-like and that the washing process for the treated cellulose was time consuming, indicating a strong alteration of the cellulose properties. The other samples were more particle-like, and the washing process was very fast. Pure glycerol was also used to pretreat the

cellulose at 150 °C for 1 h (entry 8). The appearance of the treated cellulose did not show any differences from the pristine cellulose. The glycerol-treated cellulose also easily blocked the chambers of the microfluidizer, and it was hard to obtain a stable and well-dispersed CNF suspension.

Table 1. Pretreatment conditions of cellulose in betaine hydrochloride and glycerol co-solvent.

Entry	Sample	Molar ratio	Temperature (°C)	Time (h)	Homogeneous composition
1	Bh_1Gl_6	1:6	150	1	NO
2	Bh_1Gl_3	1:3	150	1	NO
3	Bh_1Gl_2	1:2	150	1	YES
4	Bh_2Gl_3	2:3	150	1	YES
5	Bh_1Gl_2-140	1:2	140	1	NO
6	Bh_1Gl_2-130	1:2	130	1	NO
7	Bh_1Gl_2-0.5	1:2	150	0.5	NO
8	Gl-150	1	150	1	NO

Celluloses obtained from successful co-solvent treatments (Bh_1Gl_2 and Bh_2Gl_3) were used for further analysis. The morphology of the cellulose fibers before and after co-solvent treatment was imaged by SEM, as shown in **Figure 1**. The original cellulose (**Figure 1a**) consisted of long fibers with an average length of 893 μm (**Table 2**). After the pure glycerol treatment, the fibers did not show any changes (**Figure 1b**), and the resulting cellulose still contained long fibers, with an average length of 886 μm (**Table 2**). However, after the co-solvent treatment (**Figures 1c and 1d**), the fibers were degraded to short fibrous particles of about 200 μm in length (**Table 2**). This change was presumably attributed to hydrolysis of the cellulose structure caused by the hydrochloric acid released from the betaine hydrochloride at the high temperature and the depolymerization of the amorphous regions of the cellulose in the hot glycerol. The decrease in fiber length also facilitated fiber disintegration into nanocellulose and prevented chamber blocking during microfluidization. The hydrolysis of the cellulose during co-solvent pretreatment was confirmed by the DP analysis, as the DP value of the original pulp was around 3500 (Li et

al., 2017), while the DP decreased notably to below 1000 after the co-solvent treatment (**Table S1**).

The alteration of the cellulose fibers structure can be observed in the magnified SEM images (**Figures 1e, 1f, 1g, and 1h**). Compared with the original cellulose, many wrinkles could be found on the surface of the treated cellulose. The diameter of the pure glycerol-treated cellulose was close to that of the original cellulose in the wet state (**Table 2**), and the swelling was not obvious. During the co-solvent treatment, the cellulose fibers swelled and softened, and their diameter increased slightly (**Table 2**). Previously, pure glycerol pretreatment had resulted in negatively charged nanocellulose (Ramakrishnan et al., 2019), which is ascribed to the oxidation hydroxyl groups to carboxyl groups in cellulose. In the current study, the esterification reaction between the betaine hydrochloride and the hydroxyl group introduced cationic moieties on the cellulose. However, the charge densities of both sets of celluloses were quite low at ~0.05–0.06 mmol/g (**Table S1**).

(Insert Figure 1)

Table 2. The dimensions of the cellulose, determined by Valmet FS5, before and after the co-solvent treatment.

Sample	Width (μm)	Length (μm)
Original cellulose	26.88	893
Gl-150	26.55	886
Bh_1Gl_2	28.17	211
Bh_2Gl_3	30.33	183

3.2 Chemical analysis of cellulose

Changes in the cellulose chemical structure before and after the DES treatment were analyzed by DRIFTS. The spectra are shown in **Figure 2a**. The assignment of the cellulose peaks was based on previous studies (Oh et al., 2005; Proniewicz et al., 2001). The intensive broad band around 3775–3000 cm^{-1} is attributed to the stretching vibration of O-H. The other characteristic absorption peaks are the CH stretching at 2902 cm^{-1} and

the OH bending adsorbed water at 1640 cm^{-1}. The absorption bands at 1430, 1372, and 898 cm^{-1} are related to the typical cellulose structure assigned to the HCH and OCH in-plane bending vibrations, the CH deformation vibration, as well as the COC and CCO deformation modes, and the CCH stretching vibrations (Proniewicz et al., 2001). The spectra of all modified cellulose showed peaks similar to those of the original cellulose in these wavenumbers, but a new weak peak located at 1758 cm^{-1} in the DES-pretreated cellulose was also observed. This peak indicates the formation of ester groups between cellulose and betaine hydrochloride. However, the quaternary ammonium group, which should be located at around 1475 cm^{-1} (the absorption peak of the deformation vibration of C-H of CH_3 in the quaternary ammonium groups) (Ma et al., 2014) in the DES-pretreated cellulose, was not detectable, likely due to the low degree of substitution. The ester peak intensity (1758 cm^{-1}) of the nanocelluloses did not show obvious differences, indicating that the reactivity between the cellulose hydroxyl group and the betaine hydrochloride was very low without any catalyst. During the mechanical disintegration, the peak intensity related to ester group didn't decreased with the increased times of passing through microfluidizer, demonstrating the formation of stable ester bonds. This result is in accordance with the low-charge density of the modified cellulose (**Table S1**). The introduced ester group played a dual role in CNF fabrication; it served as a steric barrier to block hydrogen bonding between the molecule chains and increased the interfibrillar electrostatic repulsion. During the microfluidization process, cellulose fibrils will be easier to be liberated along the longitudinal axis of the cellulose microfibrillar structure, resulting in the successful extraction of cellulose nanoparticles.

The chemical structure of the cellulose was further elucidated using ^{13}C CP-MAS NMR spectroscopy, as shown in **Figure 2b**. The characteristic chemical shift related to carbon peaks of C1-6 remained unchanged after co-solvent treatment. The carbonyl

carbons that originated from the introduced ester groups should appear around 170–180 ppm. However, this signal was absent in the treated cellulose due to the low degree of substitution and the low sensitivity of the analysis.

(Insert Figure 2)

3.3 Morphology of nanocellulose

The morphology of cellulose nanoparticles was investigated by SEM and TEM, as illustrated in **Figure 3**. As summarized and defined in previous literature, CNFs are typically produced through mechanical refining, the nanoparticles have a higher aspect ratio with 500-2000 nm in length (Moon et al., 2011). According to SEM imaging, the samples consisted of fibrillar particles with a dimension of >500 nm in length and <30 nm in width, showing a typical structure of CNFs. The samples consisted mainly of homogeneous particles with diameters of 19.3±4.9 nm for Bh_1Gl_2 CNF I, 19.5±3.4 nm for Bh_1Gl_2 CNF II, 19.7±3.4 nm for Bh_2Gl_3 CNF I, and 17.3±3.0 nm for Bh_2Gl_3 CNF II. The diameter didn't show significant difference. The individual diameter of cellulose nanofibril should be around 3-5 nm, but due to the high interaction between the hydroxyl group and crystalline area in cellulose, it's hard to peel off cellulose bundles. TEM images also confirmed that the CNFs were structured bundles of individual nanofibrils.

(Insert Figure 3)

Previously, the birch cellulose was pretreated with urea-based DES (Sirviö et al., 2015; Li et al., 2017), and after passing through a double-chamber system (400 and 200 μm) in a microfluidizer three times at a pressure of 1300 bar, stable and homogeneous CNFs suspensions were obtained (CNF I). The diameters of CNFs were ranging from 13 to 30 nm, which is close to the CNFs in this study. However, the pressure used the current study was only 1000 bar. Although more intense mechanical treatment with smaller chambers and at higher pressure could further peel off the individual nanofibers from the

cellulose nanofibril bundles, it may also lead to the degradation of cellulose (Sirviö et al., 2015).

The mechanism of the enhancement of nanofibrillation of cellulose through this new DES treatment is ascribed to the swelling and cationization of cellulose. Hot glycerol could enter the inside of cellulose fibers, similar to urea, glycerol likely disrupted the hydrogen bond interaction between fibrils (Carrillo et al., 2014), which led to the fiber swelling, increase in surface area and promotion of nanofibrillation (Ramakrishnan et al., 2019). The fibers could be fully swelled and softened, meanwhile, glycerol could also act as delivery media of betaine hydrochloride. The swelled cellulose had an increased specific area and more exposed hydroxyl groups. Under this condition, betaine hydrochloride was more accessible to cellulose and reacted with hydroxyl groups to introduce a cationic charge on the cellulose. The formation of glyceryl glycine betaine esters between the glycerol and betaine hydrochloride likely further enhanced the swelling effect of the cellulose. Subsequently, the pretreated cellulose could be successfully disintegrated into homogeneous CNFs (**Figure 4**).

(Insert Figure 4)

After passing through the microfluidizer three times, the CNF suspension existed as a homogeneous, highly viscous, and transparent gel without any visible sedimentation or flocculation (**Figure S2**). Additional passages increased both the viscosity and transparency of the CNF gel (**Figure S3**). The appearance of the CNF suspension was similar to what was previously observed with the urea-based DESs treatments (Sirviö et al., 2015; Li et al., 2017). Another observation was that the Bh_2Gl_3 cellulose tended to easily form a stable and transparent suspension. Cellulose was fully saturated by glycerol, and the formation of glyceryl glycine betaine esters proceeded simultaneously. In this reaction, the release of hydrochloric acid worked as a catalyst, and the amount of this

catalyst could significantly affect the yield and reaction rate of the esterification. Compared with Bh_1Gl_2, Bh_2Gl_3 contained more betaine hydrochloride, which could significantly accelerate the formation of glyceryl glycine betaine esters and, in turn, enhance the swelling of the cellulose.

3.4 Crystalline structure of nanocellulose

Figure 5 presents the XRD patterns of the pristine birch cellulose and the CNF samples. All samples showed a typical diffraction pattern of cellulose I, indicating that the crystalline structure remained intact after the DES treatment. The main three 2θ diffraction angles close to 14.8°, 16.5°, and 22.7° are associated with the 1–10, 110, and 200 crystalline planes, respectively. The unchanged crystalline structure of the pretreated cellulose also demonstrated that the esterification reaction occurred mainly on the surfaces of the cellulose (Pei et al., 2013). Earlier, hot glycerol swelling also did not affect the crystalline structure of the cellulose (Ramakrishnan et al., 2019). The CrIs of CNFs were all decreased compared with the original birch cellulose. According to the method of solid-state NMR study on cellulose crystallinity (Newman, 2004), the CrI of cellulose was calculated based on sub-spectrum showing peaks assigned to the C4 in cellulose. The CrI is calculated by $CrI=I_{C4,\ cry}/(\ I_{C4,\ cry}+\ I_{C4,\ am})$ (**Figure S4**). The CrIs of birch cellulose and Bh_2Gl_3 were 55% and 50%, respectively. This result also indicated the pretreated birch cellulose showed a lower crystallinity than pristine one. The decrease of CrI of treated birch cellulose was due to the swelling effect of DES on cellulose, which was found similar as in a recent study using choline chloride and imidazole DES as swelling medium for cellulose to make cellulose nanofibers (Sirviö et al., 2020). And the further severe mechanical treatment during microfluidization may also had effect on the CrI of CNF and was noted to correlate with the number of treatment times of CNF through the microfludizer (Sirviö et al., 2015). However, the samples from different

pretreatments showed differences in CrI as a function of passages through the chambers. For Bh_1Gl_2 sample, the CrI decreased with the increased mechanical nanofibrillation, which is due to the weakening of interfibrillar hydrogen bonds and disruption on crystalline regions. For the Bh_2Gl_3 sample, the CrI in turn increased after further mechanical nanofibrillation. This result might be due more pronounced swelling in Bh_2Gl_3, the further mechanical disintegration could result in partial dissolution of less crystalline parts and decrease in nanofiber diameter. This result is in accordance with a lower diameter of nanoparticles as described in morphology analysis.

(Insert Figure 5)

3.5 Thermal stability of nanocellulose

The thermal behavior of the original cellulose and CNF samples was analyzed by TGA in a N_2 atmosphere. The results of the TGA and differential thermogravimetry analysis (DTG) curves are shown in **Figure 6**. The thermal decomposition of the cellulose could be divided into three stages: initial, main, and char decomposition. The start decomposition temperature (T_{start}), onset decomposition temperature (T_{onset}), and maximum weight-loss rate temperature (T_{max}) of the samples are listed in **Table S2**. In the initial stage, where the temperature was below T_{start}, the weight loss was due to the evaporation of the absorbed moisture. The main decomposition between approximately 200 °C and 400 °C was caused by depolymerization, dehydration of the cellulose, or decomposition of the glycosyl units. In this stage, the weight loss was very fast. The T_{max} of the original cellulose was 346 °C, which was the highest value among the five samples. The thermal stability of the cellulose was affected by its crystallinity and introduced functional groups (Lee et al., 2018; Xing et al., 2018). Consequently, the decrease in the crystallinity of the nanocellulose decreased its thermal stability. Moreover, cellulose hydrolysis during the co-solvent treatment could have lowered the thermal stability of the

nanocellulose (Hong et al., 2019a). Overall, the thermal stability of CNFs was, however, close to that of the pristine cellulose and higher than previously reported for carboxylated and sulfated nanocellulose (Sirviö et al., 2016; Li et al., 2019). This property of cellulose is very important for its application, especially when used as reinforcement in a thermoplastic composite.

(Insert Figure 6)

3.6 Mechanical properties of self-standing films

The stress-strain curves and tensile properties of the self-standing films prepared from CNFs using a filtration method are shown in **Figure 7** and **Table 3**. Generally, the films exhibited good mechanical properties with tensile strength ranging from approximately 80 to 110 MPa. These values are lower than films prepared from the CNFs of urea-based DESs pretreatment (Li et al., 2017) but are comparable to enzyme-pretreated nanocellulose films (Qing et al., 2015) (60–120 MPa). Due to the hydrolysis reaction, the DP of glycerol and betaine hydrochloride co-solvent treated cellulose is lower than that of the urea-based DES pretreatment samples. Therefore, the length of the resulting nanofibers was shorter than in the previous studies. The long fibers with high aspect ratio nanocellulose result mostly in films with good mechanical properties (Saito et al., 2009), which could be ascribed to the possibility for stronger nanoparticle interconnection induced by the entanglement of the flexible cellulose nanofibers (Dufresne, 2017). One-way ANOVA analysis was performed to evaluate the statistical differences of the mechanical measurements (OriginPro 2018). The analysis did not show any significant differences between the tensile strength of the nanocellulose films at $p<0.05$ (the p-value was 0.213). However, it was confirmed by elongation at break values during the mechanical tests that the films prepared from CNF II were slightly brittler than

417 the CNF I films. Probably, the prolonged mechanical treatment decreased the DP of the
418 cellulose and resulted in brittler films (Sirviö et al., 2015).

419 **(Insert Figure 7)**

420 **Table 3.** Mechanical properties of the CNF films.

Sample	Elastic modulus (GPa)	Maximum tensile strength (MPa)	Elongation at break (%)
Bh_1Gl_2 CNF Ⅰ	4.3±1.3	86±6	3.6±0.2
Bh_1Gl_2 CNF Ⅱ	5.5±0.7	93±13	3.1±0.5
Bh_2Gl_3 CNF Ⅰ	4.4±1.2	99±5	4.4±1.2
Bh_2Gl_3 CNF Ⅱ	5.3±0.8	93±7	3.1±0.7

421 ## 4. Conclusions

422 Cellulose pulp was pretreated in glycerol and betaine hydrochloride co-solvent under
423 various conditions, with a maximum mass yield of 72.5 wt-%. After mechanical
424 disintegration, highly viscous and transparent CNF suspensions were obtained. The molar
425 ratio of betaine hydrochloride to glycerol was a crucial factor for cellulose modification.
426 Cellulose pretreated with a Bh:Gl mole ratio above 1:2 could be successfully
427 disintegrated into CNF. The glycerol functioned as a swelling agent and reaction medium
428 for betaine hydrochloride, and it weakened the interfibrillar hydrogen bonding of the
429 cellulose. Moreover, the cationization of the glycerol and cellulose increased the
430 electrostatic repulsion within the cellulose, which further facilitated cellulose swelling.
431 The cellulose's degree of substitution with the betaine hydrochloride ester was very low,
432 and the CNFs possessed only a low cationic charge density. The obtained nanofibers were
433 17–20 nm in diameter, with degree of crystallinity ranging from 67.7 to 74.4%. The
434 thermal stability of the obtained nanocellulose was comparable to that of the original
435 cellulose. In addition, the nanostructured self-standing nanocellulose films showed good
436 mechanical performance, with their tensile strength ranging from 80 to 110 MPa. Overall,
437 the chemicals used are naturally available, cheap, safe, and biodegradable. The current

study presented a new green and efficient route for producing CNFs with a swelling treatment.

ACKNOWLEDGMENT

This research was supported by grants from the National Natural Science Foundation of China (31370567), the Doctorate Fellowship Foundation of Nanjing Forestry University, the National First-Class Disciplines, the Priority Academic Program Development of Jiangsu Higher Education Institutions, and the Academy of Finland project “Bionanochemicals” (No. 298295).

References

Abbott, A.P., Capper, G., Davies, D.L., Rasheed, R., 2004. Ionic liquids based upon metal halide/substituted quaternary ammonium salt mixtures. Inorg. Chem. 43, 3447–3452. https://doi.org/10.1021/ic049931s

Bhatnagar, A., Sain, M., 2005. Processing of cellulose nanofiber-reinforced composites. J. Reinf. Plast. Comp. 24, 1259–1268. https://doi.org/10.1177/0731684405049864

Braun, B., Dorgan, J.R., 2009. Single-Step Method for the Isolation and Surface Functionalization of Cellulosic Nanowhiskers. Biomacromolecules 10, 334–341. https://doi.org/10.1021/bm8011117

Carrillo, C.A., Laine, J., Rojas, O.J., 2014. Microemulsion Systems for Fiber Deconstruction into Cellulose Nanofibrils. ACS Appl. Mater. Interfaces 6, 22622–22627. https://doi.org/10.1021/am5067332

Carvalho, D.M. de, Moser, C., Lindström, M.E., Sevastyanova, O., 2019. Impact of the chemical composition of cellulosic materials on the nanofibrillation process and nanopaper properties. Ind. Crop. Prod. 127, 203–211. https://doi.org/10.1016/j.indcrop.2018.10.052

Chen, C., Li, D., Abe, K., Yano, H., 2018a. Formation of high strength double-network gels from cellulose nanofiber/polyacrylamide via NaOH gelation treatment. Cellulose 25, 5089–5097. https://doi.org/10.1007/s10570-018-1938-5

Chen, C., Mo, M., Chen, W., Pan, M., Xu, Z., Wang, H., Li, D., 2018b. Highly conductive nanocomposites based on cellulose nanofiber networks via NaOH treatments. Composites Science and Technology 156, 103–108. https://doi.org/10.1016/j.compscitech.2017.12.029

Chen, C., Wang, H., Li, S., Fang, L., Li, D., 2017. Reinforcement of cellulose nanofibers in polyacrylamide gels. Cellulose 24, 5487–5493. https://doi.org/10.1007/s10570-017-1512-6

Dufresne, A., 2017. Cellulose nanomaterial reinforced polymer nanocomposites. Curr. Opin. Colloid Interface Sci. 29, 1–8. https://doi.org/10.1016/j.cocis.2017.01.004

Habibi, Y., Lucia, L.A., Rojas, O.J., 2010. Cellulose nanocrystals: chemistry, self-assembly, and applications. Chem. Rev. 110, 3479–3500. https://doi.org/10.1021/cr900339w

Hong, S., Song, Y., Yuan, Y., Lian, H., Liimatainen, H., 2020a. Production and characterization of lignin containing nanocellulose from luffa through an acidic deep eutectic solvent treatment and systematic fractionation. Ind. Crop. Prod. 143, 111913. https://doi.org/10.1016/j.indcrop.2019.111913

Hong, S., Yang, Q., Yuan, Y., Chen, L., Song, Y., Lian, H., 2019a. Sustainable co-solvent induced one step extraction of low molecular weight chitin with high purity from raw lobster shell. Carbohydr. Polym. 205, 236–243. https://doi.org/10.1016/j.carbpol.2018.10.045

Hong, S., Yuan, Y., Liu, C., Chen, W., Chen, L., Lian, H., Liimatainen, H., 2020b. A stretchable and compressible ion gel based on a deep eutectic solvent applied as a strain sensor and electrolyte for supercapacitors. J. Mater. Chem. C 8, 550–560. https://doi.org/10.1039/C9TC05913J

Hong, S., Yuan, Y., Yang, Q., Chen, L., Deng, J., Chen, W., Lian, H., Mota-Morales, J.D., Liimatainen, H., 2019b. Choline chloride-zinc chloride deep eutectic solvent mediated preparation of partial O-acetylation of chitin nanocrystal in one step reaction. Carbohydr. Polym. 220, 211–218. https://doi.org/10.1016/j.carbpol.2019.05.075

Hong, S., Yuan, Y., Yang, Q., Zhu, P., Lian, H., 2018. Versatile acid base sustainable solvent for fast extraction of various molecular weight chitin from lobster shell. Carbohydr. Polym. 201, 211–217. https://doi.org/10.1016/j.carbpol.2018.08.059

Journoux-Lapp, C., Vigier, K.D.O., Bachmann, C., Marinkovic, S., Estrine, B., Frapper, G., Jerome, F., 2017. Elucidation of the role of betaine hydrochloride in glycerol esterification: towards bio-based ionic building blocks. Green Chem. 19, 5647–5652. https://doi.org/10.1039/c7gc02767b

Laitinen, O., Ojala, J., Sirviö, J.A., Liimatainen, H., 2017. Sustainable stabilization of oil in water emulsions by cellulose nanocrystals synthesized from deep eutectic solvents. Cellulose 24, 1679–1689. https://doi.org/10.1007/s10570-017-1226-9

Lee, H., Sundaram, J., Zhu, L., Zhao, Y., Mani, S., 2018. Improved thermal stability of cellulose nanofibrils using low-concentration alkaline pretreatment. Carbohydr. Polym. 181, 506–513. https://doi.org/10.1016/j.carbpol.2017.08.119

Li, P., Sirvio, J.A., Haapala, A., Liimatainen, H., 2017. Cellulose nanofibrils from nonderivatizing urea-based deep eutectic solvent pretreatments. ACS Appl. Mater. Interfaces 9, 2846–2855. https://doi.org/10.1021/acsami.6b13625

Li, P., Sirviö, J.A., Hong, S., Ammala, A., Llimatainen, H., 2019. Preparation of flame-retardant lignin-containing wood nanofibers using a high-consistency mechano-chemical pretreatment. Chem. Eng. J. 375, 122050. https://doi.org/10.1016/j.cej.2019.122050

Li, Y., Zhu, H., Shen, F., Wan, J., Lacey, S., Fang, Z., Dai, H., Hu, L., 2015. Nanocellulose as green dispersant for two-dimensional energy materials. Nano Energy 13, 346–354. https://doi.org/10.1016/j.nanoen.2015.02.015

Liimatainen, H., Sirvio, J., Haapala, A., Hormi, O., Niinimaki, J., 2011. Characterization of highly accessible cellulose microfibers generated by wet stirred media milling. Carbohydr. Polym. 83, 2005–2010. https://doi.org/10.1016/j.carbpol.2010.11.007

Liimatainen, H., Sirvio, J., Pajari, H., Hormi, O., Niinimaki, J., 2013. Regeneration and recycling of aqueous periodate solution in dialdehyde cellulose production. J. Wood Chem. Technol. 33, 258–266. https://doi.org/10.1080/02773813.2013.783076

Liimatainen, H., Visanko, M., Sirviö, J.A., Hormi, O.E.O., Niinimaki, J., 2012. Enhancement of the nanofibrillation of wood cellulose through sequential periodate–chlorite oxidation. Biomacromolecules 13, 1592–1597. https://doi.org/10.1021/bm300319m

Lin, N., Dufresne, A., 2014. Nanocellulose in biomedicine: Current status and future prospect. Eur. Polym. J. 59, 302–325. https://doi.org/10.1016/j.eurpolymj.2014.07.025

Lu, Y., Yu, J., Ma, J., Wang, Z., Fan, Y., Zhou, X., 2019. High-yield preparation of cellulose nanofiber by small quantity acid assisted milling in glycerol. Cellulose 26, 3735–3745. https://doi.org/10.1007/s10570-019-02335-x

Ma, W., Yan, S., Meng, M., Zhang, S., 2014. Preparation of betaine-modified cationic cellulose and its application in the treatment of reactive dye wastewater. J. Appl. Polym. Sci. 131, 40522. https://doi.org/10.1002/app.40522

Moon, R.J., Martini, A., Nairn, J., Simonsen, J., Youngblood, J., 2011. Cellulose nanomaterials review: structure, properties and nanocomposites. Chem. Soc. Rev. 40, 3941. https://doi.org/10.1039/c0cs00108b

Mota-Morales, J.D., Sánchez-Leija, R.J., Carranza, A., Pojman, J.A., del Monte, F., Luna-Bárcenas, G., 2018. Free-radical polymerizations of and in deep eutectic solvents: Green synthesis of functional materials. Prog. Polym. Sci. 78, 139–153. https://doi.org/10.1016/j.progpolymsci.2017.09.005

Newman, R.H., 2004. Homogeneity in cellulose crystallinity between samples of Pinus radiata wood. Holzforschung 58, 91–96. https://doi.org/10.1515/HF.2004.012

Oh, S.Y., Yoo, D.I., Shin, Y., Seo, G., 2005. FTIR analysis of cellulose treated with sodium hydroxide and carbon dioxide. Carbohydr. Res. 340, 417–428. https://doi.org/10.1016/j.carres.2004.11.027

Ojala, J., Sirvio, J.A., Liimatainen, H., 2016. Nanoparticle emulsifiers based on bifunctionalized cellulose nanocrystals as marine diesel oil-water emulsion stabilizers. Chem. Eng. J. 288, 312–320. https://doi.org/10.1016/j.cej.2015.10.113

Pääkkö, M., Ankerfors, M., Kosonen, H., Nykänen, A., Ahola, S., Österberg, M., Ruokolainen, J., Laine, J., Larsson, P.T., Ikkala, O., Lindström, T., 2007. Enzymatic Hydrolysis Combined with Mechanical Shearing and High-Pressure Homogenization for Nanoscale Cellulose Fibrils and Strong Gels. Biomacromolecules 8, 1934–1941. https://doi.org/10.1021/bm061215p

Pei, A., Butchosa, N., Berglund, L.A., Zhou, Q., 2013. Surface quaternized cellulose nanofibrils with high water absorbency and adsorption capacity for anionic dyes. Soft Matter 9, 2047–2055. https://doi.org/10.1039/c2sm27344f

Proniewicz, L.M., Paluszkiewicz, C., Weselucha-Birczynska, A., Majcherczyk, H., Baranski, A., Konieczna, A., 2001. FT-IR and FT-Raman study of hydrothermally degradated cellulose. J. Mol. Struct. 596, 163–169. https://doi.org/10.1016/S0022-2860(01)00706-2

Qing, Y., Sabo, R., Wu, Y., Zhu, J.Y., Cai, Z., 2015. Self-assembled optically transparent cellulose nanofibril films: effect of nanofibril morphology and drying procedure. Cellulose 22, 1091–1102. https://doi.org/10.1007/s10570-015-0563-9

Ramakrishnan, A., Ravishankar, K., Dhamodharan, R., 2019. Preparation of nanofibrillated cellulose and nanocrystalline cellulose from surgical cotton and cellulose pulp in hot-glycerol medium. Cellulose 26, 3127–3141. https://doi.org/10.1007/s10570-019-02312-4

Saito, T., Hirota, M., Tamura, N., Kimura, S., Fukuzumi, H., Heux, L., Isogai, A., 2009. Individualization of nano-sized plant cellulose fibrils by direct surface carboxylation using TEMPO catalyst under neutral conditions. Biomacromolecules 10, 1992–1996. https://doi.org/10.1021/bm900414t

Saito, T., Nishiyama, Y., Putaux, J.-L., Vignon, M., Isogai, A., 2006. Homogeneous Suspensions of Individualized Microfibrils from TEMPO-Catalyzed Oxidation of Native Cellulose. Biomacromolecules 7, 1687–1691. https://doi.org/10.1021/bm060154s

Segal, L., Creely, J.J., Martin, A.E., Conrad, C.M., 1959. An empirical method for estimating the degree of crystallinity of native cellulose using the X-Ray diffractometer. Text. Res. J. 29, 786–794. https://doi.org/10.1177/004051755902901003

Siró, I., Plackett, D., 2010a. Microfibrillated cellulose and new nanocomposite materials: a review. Cellulose 17, 459–494. https://doi.org/10.1007/s10570-010-9405-y

Siró, I., Plackett, D., 2010b. Microfibrillated cellulose and new nanocomposite materials: a review. Cellulose 17, 459–494. https://doi.org/10.1007/s10570-010-9405-y

Sirviö, J.A., 2019. Fabrication of regenerated cellulose nanoparticles by mechanical disintegration of cellulose after dissolution and regeneration from a deep eutectic solvent. J. Mater. Chem. A 7, 755–763. https://doi.org/10.1039/C8TA09959F

Sirviö, J.A., Hyypiö, K., Asaadi, S., Junka, K., Liimatainen, H., 2020. High-strength cellulose nanofibers produced via swelling pretreatment based on a choline chloride–imidazole deep eutectic solvent. Green Chem. 22, 1763–1775. https://doi.org/10.1039/C9GC04119B

Sirviö, J.A., Liimatainen, H., Visanko, M., Niinimaki, J., 2014. Optimization of dicarboxylic acid cellulose synthesis: Reaction stoichiometry and role of hypochlorite scavengers. Carbohydr. Polym. 114, 73–77. https://doi.org/10.1016/j.carbpol.2014.07.081

Sirviö, J.A., Visanko, M., Liimatainen, H., 2016. Acidic deep eutectic solvents as hydrolytic media for cellulose nanocrystal production. Biomacromolecules 17, 3025–3032. https://doi.org/10.1021/acs.biomac.6b00910

Sirviö, J.A., Visanko, M., Liimatainen, H., 2015. Deep eutectic solvent system based on choline chloride-urea as a pre-treatment for nanofibrillation of wood cellulose. Green Chem. 17, 3401–3406. https://doi.org/10.1039/C5GC00398A

Smith, E.L., Abbott, A.P., Ryder, K.S., 2014. Deep eutectic solvents (DESs) and their applications. Chem. Rev. 114, 11060–11082. https://doi.org/10.1021/cr300162p

Suopajärvi, T., Ricci, P., Karvonen, V., Ottolina, G., Liimatainen, H., 2020. Acidic and alkaline deep eutectic solvents in delignification and nanofibrillation of corn stalk, wheat straw, and rapeseed stem residues. Ind. Crop. Prod. 145, 111956. https://doi.org/10.1016/j.indcrop.2019.111956

Vigier, K.D.O., Benguerba, A., Barrault, J., Jerome, F., 2012. Conversion of fructose and inulin to 5-hydroxymethylfurfural in sustainable betaine hydrochloride-based media. Green Chem. 14, 285–289. https://doi.org/10.1039/c1gc16236e

Vigier, K.D.O., Chatel, G., Jerome, F., 2015. Contribution of deep eutectic solvents for biomass processing: opportunities, challenges, and limitations. ChemCatChem 7, 1250–1260. https://doi.org/10.1002/cctc.201500134

Willberg-Keyriläinen, P., Hiltunen, J., Ropponen, J., 2018. Production of cellulose carbamate using urea-based deep eutectic solvents. Cellulose 25, 195–204. https://doi.org/10.1007/s10570-017-1465-9

608 Wu, C.-N., Saito, T., Fujisawa, S., Fukuzumi, H., Isogai, A., 2012. Ultrastrong and High Gas-
609 Barrier Nanocellulose/Clay-Layered Composites. Biomacromolecules 13, 1927–1932.
610 https://doi.org/10.1021/bm300465d
611 Xing, L., Gu, J., Zhang, W., Tu, D., Hu, C., 2018. Cellulose I and II nanocrystals produced by
612 sulfuric acid hydrolysis of Tetra pak cellulose I. Carbohydr. Polym. 192, 184–192.
613 https://doi.org/10.1016/j.carbpol.2018.03.042
614 Zdanowicz, M., Wilpiszewska, K., Spychaj, T., 2018. Deep eutectic solvents for polysaccharides
615 processing. A review. Carbohydr. Polym. 200, 361–380.
616 https://doi.org/10.1016/j.carbpol.2018.07.078
617

Enhancement of the nanofibrillation of birch cellulose pretreated with natural deep eutectic solvent

Shu Hong,[a, b] *Yang Yuan,*[a] *Panpan Li,*[b] *Kaitao Zhang,*[b] *Hailan Lian,*[*, a] *Henrikki Liimatainen* [*, b]

[a] College of Materials Science and Engineering, Nanjing Forestry University, Nanjing, 210037, China

[b] Fibre and Particle Engineering Research Unit, University of Oulu, P.O. Box 4300, 90014 Oulu, Finland

* Corresponding authors

Hailan Lian, E-mail: lianhailan@njfu.edu.cn and Henrikki Liimatainen, E-mail: Henrikki.Liimatainen@oulu.fi

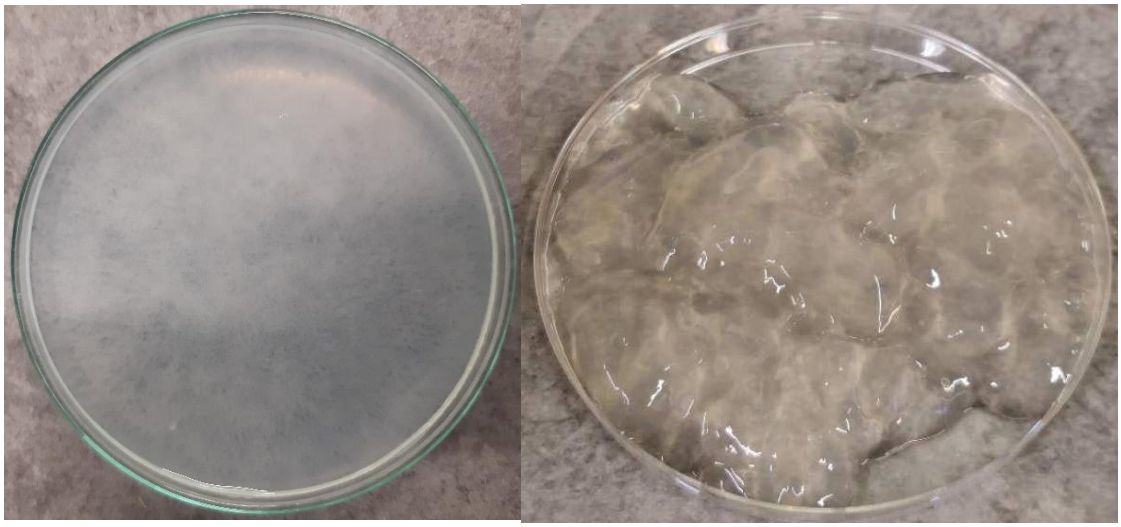

Figure S1. Appearance of typical unsuccessful treatments that showed obviously inhomogeneous suspension, a lot of visible cellulose particles and flocculation (left). And typical appearance of samples from the successful treatments was homogeneous, transparent and highly viscous (right).

Figure S2. Appearance of 0.5% cellulose nanofibers suspensions, from left to right were Bh_1Gl_2 CNF Ⅰ, Bh_1Gl_2 CNF Ⅱ, Bh_2Gl_3 CNF Ⅰ, and Bh_2Gl_3 CNF Ⅱ.

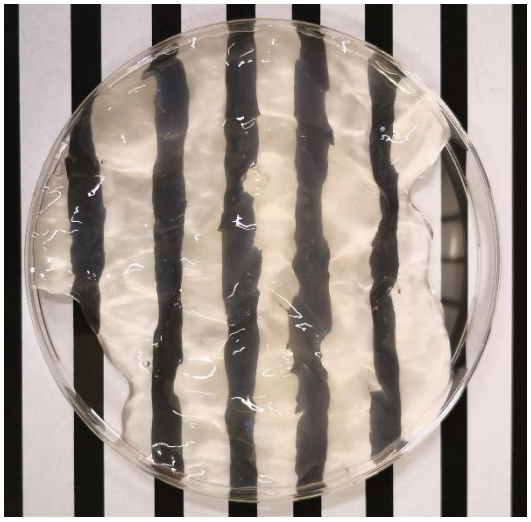

Figure S3. Appearance of 0.5% cellulose nanofiber suspension of Bh_2Gl_3 CNF Ⅱ spread in petri dish.

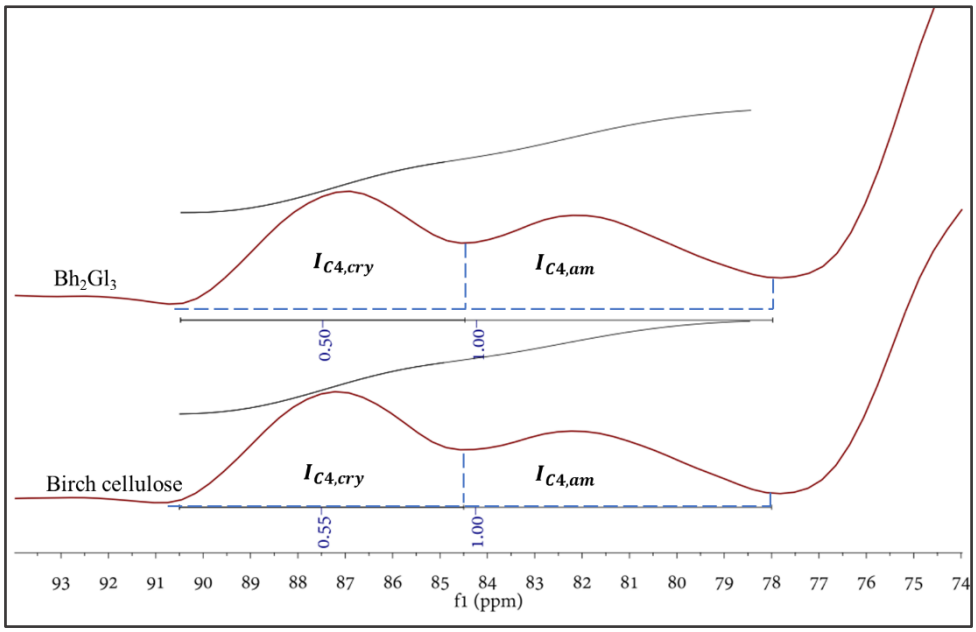

Figure S4. CrI calculation of C4 region in NMR for birch cellulose and Bh_2Gl_3.

Table S1. Yield, surface charge density and degree of polymerization of cellulose after co-solvent pretreatment.

Sample	Yield (%)	Cationic charge density (mmol/g)	DP
Bh_1Gl_2	72.5	0.05 ± 0.01	780
Bh_2Gl_3	70.3	0.06 ± 0.01	690

Table S2. Thermal degradation data of birch cellulose and obtained cellulose nanofibers.

Sample	T_{start} (°C)	T_{onset} (°C)	T_{max} (°C)
Birch cellulose	211	326	346
Bh_1Gl_2 CNF Ⅰ	203	319	339
Bh_1Gl_2 CNF Ⅱ	207	318	341
Bh_2Gl_3 CNF Ⅰ	218	319	341
Bh_2Gl_3 CNF Ⅱ	220	321	341

List of Figures

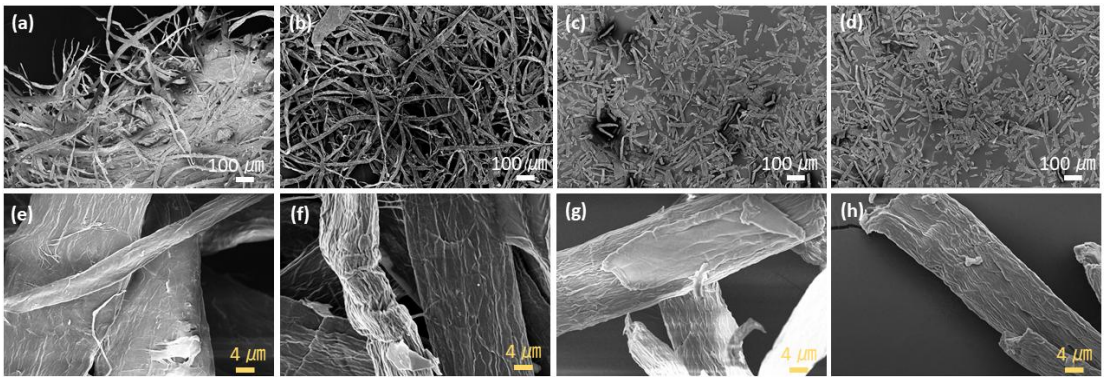

Figure 1. SEM images with different magnification of birch cellulose, (a) x200 and (e) x5000 SE; pretreated cellulose using pure glycerol, (b) x200 and (f) x5000 SE; Bh:Gl mole ratio of 1:2 (entry 3 in Table 1), (c) x200 and (g) x5000 SE; and pretreated cellulose using a Bh:Gl mole ratio of 2:3 (entry 4 in Table 1), (d) x200 and (h) x5000 SE.

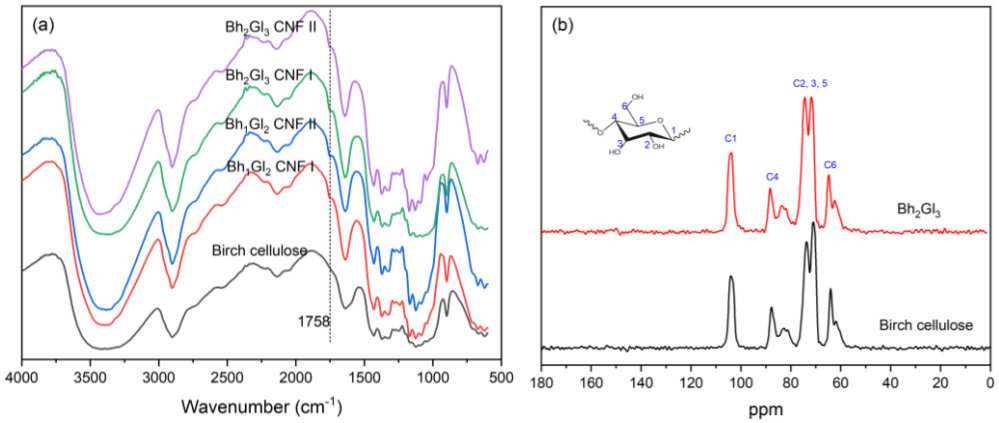

Figure 2. (a) DRIFT and (b) NMR spectra of birch cellulose and nanocelluloses.

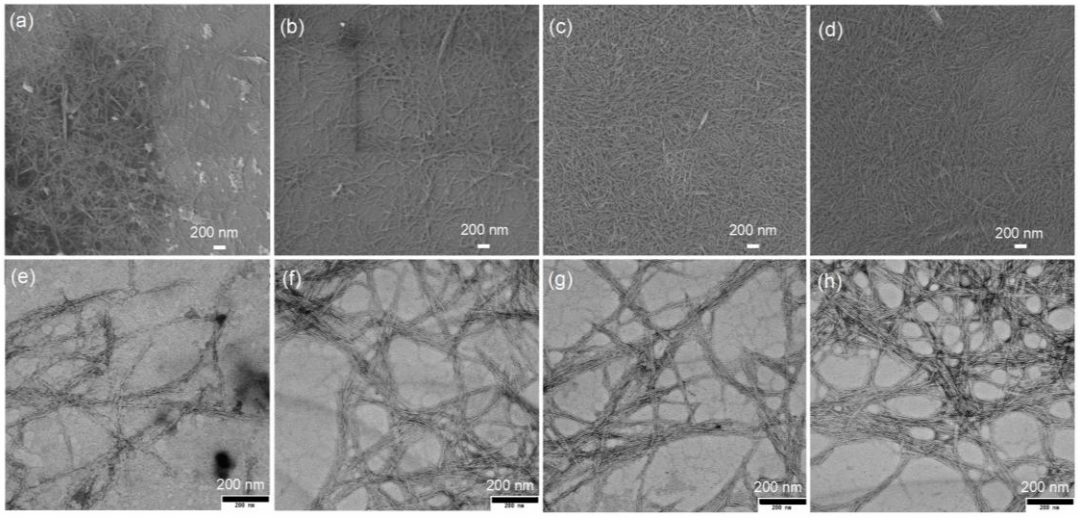

Figure 3. SEM and TEM images of nanocelluloses: (a, e) Bh_1Gl_2 CNF I, (b, f) Bh_1Gl_2 CNF II, (c, g) Bh_2Gl_3 CNF I, and (e, h) Bh_2Gl_3 CNF II.

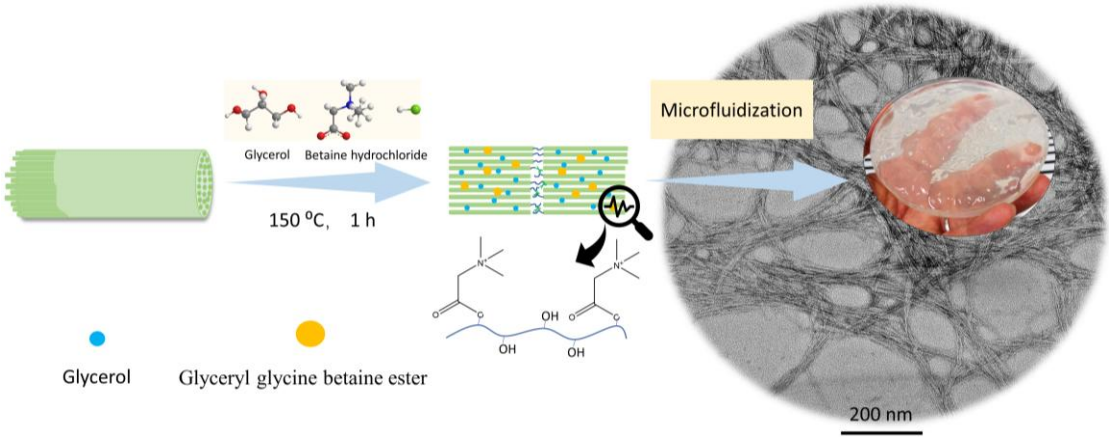

Figure 4. Mechanistic illustration for the preparation of CNF based on betaine hydrochloride and glycerol co-solvent pretreatment.

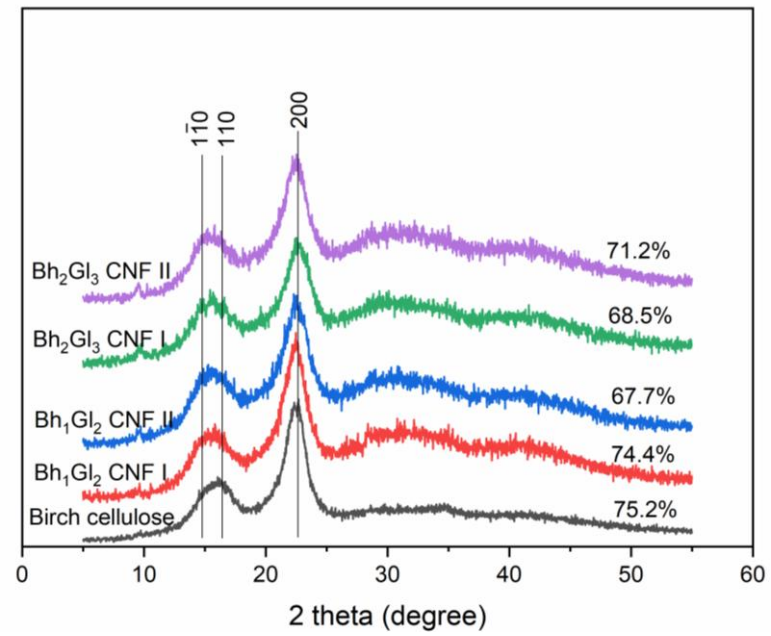

Figure 5. XRD diffraction patterns of the pristine cellulose and CNFs.

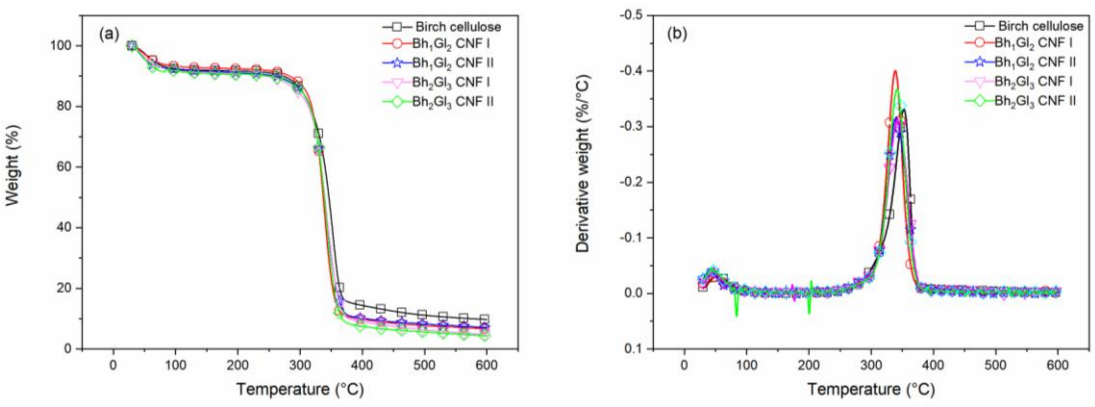

Figure 6. (a) TGA and (b) DTG curves of the pristine cellulose and CNFs.

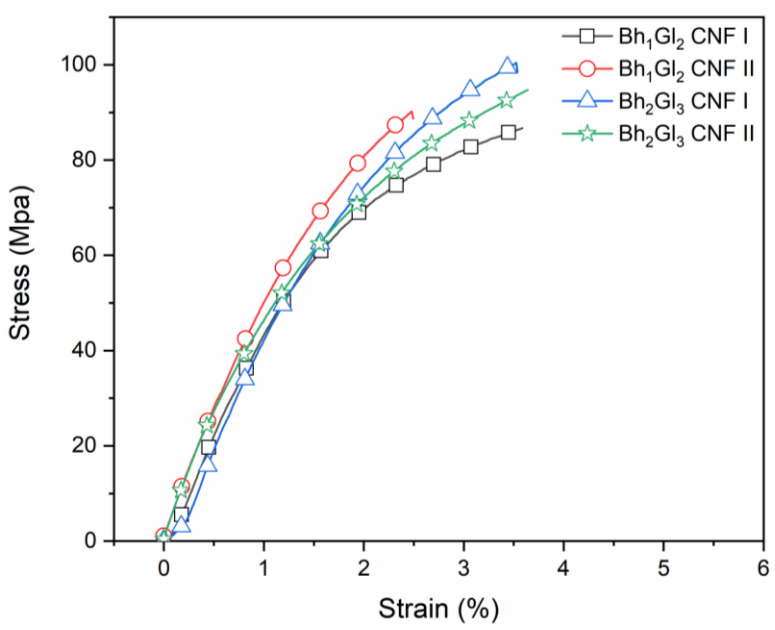

Figure 7. Typical tensile stress-strain curves of the CNF films.

***Credit Author Statement**

Shu Hong: Original draft preparation, Conceptualization, Methodology, Software. **Yang Yuan**: Data curation, Software, Conceptualization. **Panpan Li**: Investigation, Methodology. **Kaitao Zhang:** Formal analysis, Investigation. **Hailan Lian**: Supervision, Project administration. **Henrikki Liimatainen:** Resources, Supervision, Project administration, Writing- Reviewing and Editing.

***Declaration of Interest Statement**

Declaration of interests

☒ The authors declare that they have no known competing financial interests or personal relationships that could have appeared to influence the work reported in this paper.

☐The authors declare the following financial interests/personal relationships which may be considered as potential competing interests: